

Capacitively coupled quantum dots as a single-electron switch

I.H. Chan^a, P. Fallahi^a, R.M. Westervelt^{a,*}, K.D. Maranowski^b, A.C. Gossard^b

^a*Division of Engineering and Applied Sciences, Harvard University, Cambridge, MA 02138, USA*

^b*Materials Department, University of California at Santa Barbara, Santa Barbara, CA 93106, USA*

Abstract

A double quantum dot in a GaAs/AlGaAs heterostructure with strong interdot capacitance but no interdot tunneling can be constructed using a floating metal gate that covers both dots and an etched trench between the dots that prevents tunneling. The interdot capacitance $C_{\text{INT}} = 0.34C_{\Sigma}$ between Dots 1 and 2, measured using the Coulomb blockade, was significantly larger than that measured for similar dots without a floating gate. When a single electron is added to Dot 1 the charge couples to Dot 2, and vice versa, causing the Coulomb blockade peaks to split. The change in dot conductance from peak splitting can be as large as two orders of magnitude, allowing the double dot to be used as a single-electron switch. The split conductance peaks observed for weak tunneling from each dot to its leads were fit by a thermally broadened line shape, and good agreement with the data was found. Charge fluctuations induced by stronger tunneling from Dot 2 to its leads softened the splitting transition on Dot 1 that was maintained in the weak tunneling regime. Under the same conditions the splitting for Dot 2 remained sharp.

© 2002 Elsevier Science B.V. All rights reserved.

Keywords: Quantum dots; Coulomb blockade; Single-electronics; Switch

1. Introduction

Quantum dots have been studied extensively [1–3] and the effect of tunneling on the Coulomb blockade behavior in a double-dot system is well understood [4–9]. We turn to explore the Coulomb blockade behavior of a capacitively coupled double quantum dot system in which there is no tunneling between the dots [10]. While there have been experiments that used capacitively coupled dots to measure the charge of a device [11], they were operated in the linear regime where the conductance of the dot was

essentially a linear function of the charge being measured. This paper describes the Coulomb blockade behavior of a strongly capacitively coupled quantum dot system, and shows how its non-linear conductance versus charge behavior can be employed as a single-electron switch. Single-electron switches may be used in logic circuits and possible implementations of quantum information processing.

2. Device

The device used in this experiment is shown in Fig. 1(a) together with a schematic of the coupled dots in perspective (Fig. 1(b)). The device was made in a two-dimensional electron gas (2DEG) inside a GaAs/AlGaAs heterostructure using electron-beam

* Corresponding author. Tel.: +1-617-495-3296; fax: +1-617-495-9837.

E-mail address: westervelt@deas.harvard.edu
(R.M. Westervelt).

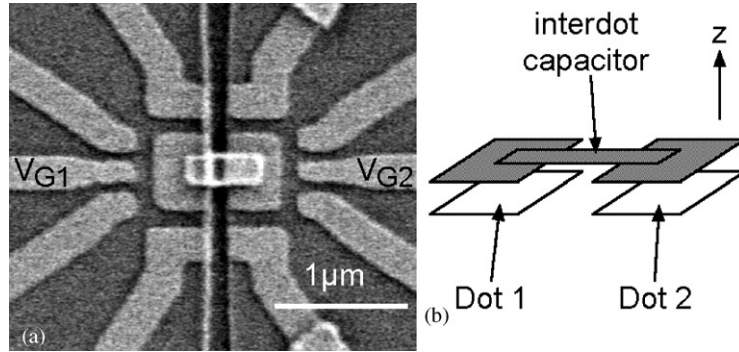


Fig. 1. (a) Scanning electron micrograph of the capacitively coupled quantum dots. The device consists of two laterally defined quantum dots in a GaAs/AlGaAs heterostructure separated from each other by an etched trench (dark vertical line) to prevent tunneling. Capacitive coupling between the dots is enhanced by an interdot capacitor which spans the etched trench. (b) Schematic showing the quantum dots and the interdot capacitor in perspective.

lithography. Two nominally identical quantum dots are formed on either side of an etched trench (the dark vertical line in Fig. 1(a)) using the split-gate technique. The etched trench separates the two dots and no tunneling was observed between the dots. The interdot capacitor structure consists of a metal plate above each dot joined together across the etched trench by a metal bridge. The resulting device consists of two separately contactable quantum dots (parallel quantum dots) with strong capacitive coupling and no tunnel coupling.

The 2DEG had a mobility $\mu = 5 \times 10^5 \text{ cm}^2/\text{V s}$ and a density $n = 3 \times 10^{11} \text{ cm}^{-2}$, and was located 57 nm below the surface of the heterostructure. The conductance of each dot was measured separately using standard lock-in techniques at different frequencies. All measurements were done in a dilution refrigerator at a base temperature of 10 mK and a measured electron temperature of 70 mK ($k_B T = 6 \text{ } \mu\text{eV}$).

3. Peak splitting

Figs. 2(a) and (b) show the conductances of Dots 1 and 2, respectively, as a function of the change in side gate voltage ΔV_{G1} of Dot 1 and the change in side gate voltage ΔV_{G2} of Dot 2. Both dots are weakly tunnel coupled to their leads for this measurement and the thermally smeared Coulomb blockade peaks of each dot are visible. Also visible are the ‘splits’ or ‘breaks’ in the Coulomb blockade peaks that occur whenever

both dots exhibit Coulomb blockade peaks. Fig. 2(c) shows the superimposition of Figs. 2(a) and (b) to illustrate the relative positions of each dot’s Coulomb blockade peaks. The Coulomb blockade peak splitting in one dot is due to the charge from an additional electron in the adjacent dot shifting the peaks laterally. The superimposed Coulomb blockade peaks in Fig. 2(c) display the hexagonal pattern that is characteristic of a coupled double dot system [6–8,12]. The amount of peak splitting ΔV_S relative to the double dot period ΔV_P is a measure of the interdot capacitance C_{INT} between the two quantum dots [12]:

$$C_{\text{INT}} = \frac{2\Delta V_S}{\Delta V_P} C_\Sigma,$$

where C_Σ is the single-dot capacitance. The small cross-capacitances between each dot and the opposite side gate shear the conductance pattern in Fig. 2 but do not alter the measured value of C_{INT} .

The single-dot capacitance C_Σ was measured by applying a finite source-drain bias across Dot 2 and varying V_{G2} to obtain the Coulomb diamond of Fig. 3. During this measurement, Dot 1 was formed and in the Coulomb blockade regime, but no change in its charge state occurred during the measurement. It is necessary to measure C_Σ with Dot 1 formed in order to obtain the single-dot capacitance that exists within the double-dot system. The measured single-dot charging energy $E_C \equiv e^2/C_\Sigma = 380 \pm 20 \text{ } \mu\text{eV}$, giving a single-dot capacitance $C_\Sigma = 420 \pm 20 \text{ aF}$. From Fig. 2(c) the peak splitting $\Delta V_S/\Delta V_P = 0.17 \pm 0.01$,

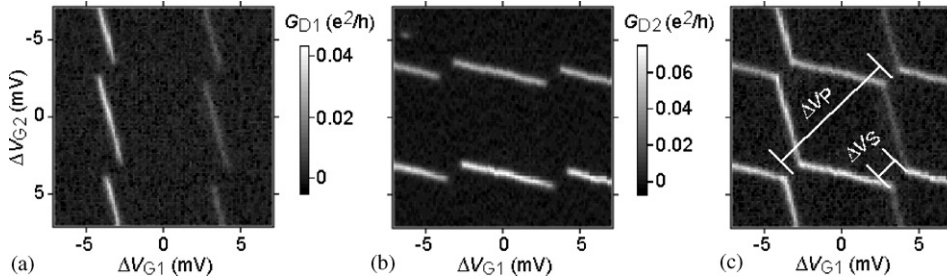


Fig. 2. Coulomb blockade peaks of (a) Dot 1 and (b) Dot 2 as a function of side gate voltages. (c) Superimposition of (a) and (b), showing that the peaks split when both dots are simultaneously on Coulomb blockade peaks. The amount of interdot capacitance is indicated by the ratio of the peak splitting ΔV_S to the double dot period ΔV_P .

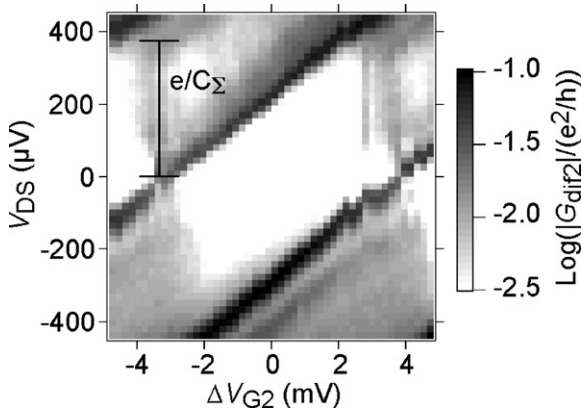


Fig. 3. Log of the differential conductance of Dot 2 as a function of Dot 2's side gate voltage and drain-source bias, displaying a Coulomb diamond. The measurement was made with Dot 1 formed but with no change in its charge observed.

giving $C_{INT}/C_\Sigma = 0.34 \pm 0.02$, which is significantly larger than for capacitively coupled lateral quantum dots previously studied [8,11].

4. Switching behavior

Fig. 4 shows how a single electron in Dot 1 turns the conductance of Dot 2 on and off. The inset shows the Coulomb blockade peaks of both dots superimposed and the white line in the inset shows the range of V_G covered. The gate voltage V_G is the linear combination of V_{G1} and V_{G2} parallel to the Coulomb blockade peaks of Dot 2. This means that changing V_G induces charge in Dot 1 only, and does nothing to

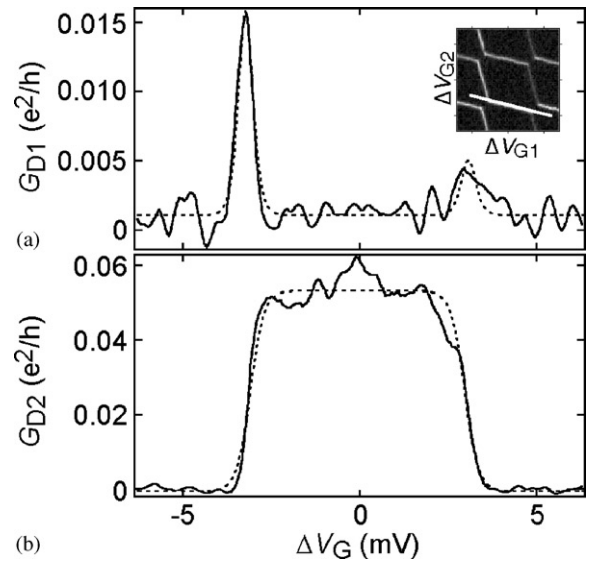


Fig. 4. Conductances of (a) Dot 1 and (b) Dot 2 along the white line indicated in the inset. ΔV_G is the combination of ΔV_{G1} and ΔV_{G2} that is parallel to the Coulomb blockade peaks of Dot 2. As single electrons are added to Dot 1, the conductance of Dot 2 is switched from off to on and back to off.

Dot 2. Fig. 4(a) shows two Coulomb blockade peaks (the second, near $\Delta V_G = 3$ mV, is just visible), indicating the introduction of a single electron into Dot 1. In response to these changes in charge on Dot 1, the conductance of Dot 2 switches on, and then off (Fig. 4(b)). This switching behavior is made possible by the large capacitive coupling between the dots that allows an electron in one dot to shift the Coulomb blockade peak of another dot by several times its

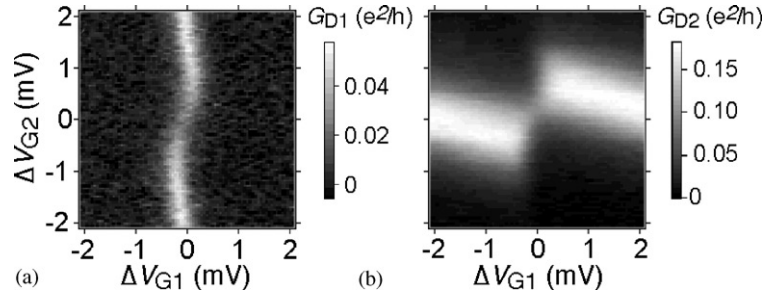


Fig. 5. Conductances of (a) Dot 1, which is weakly coupled to its leads, and (b) Dot 2, which is strongly coupled to its leads, around the peak splitting. The abruptness of the peak splitting in one dot is determined by the Coulomb blockade peak width of the other dot. Hence the peak splitting of Dot 2 in (b) is abrupt while that for Dot 1 in (a) is smooth.

thermally smeared width so as to move the dot completely on or off a Coulomb blockade peak. The role of Dot 1 as the ‘trigger’ dot and Dot 2 as the ‘switched’ dot can be reversed by making V_G parallel to the Coulomb blockade peaks of Dot 1 instead.

The dashed lines in Fig. 4 are fits of theory to the data. In Fig. 4(a), two thermally smeared Coulomb blockade peaks [2] with the same widths are fit to the data:

$$G_{D1}(\Delta V_G) = G_{D10} + \frac{\delta G_{D11}}{\cosh^2(a(\Delta V_G - \Delta V_{G11}))} + \frac{\delta G_{D12}}{\cosh^2(a(\Delta V_G - \Delta V_{G12}))},$$

where the conductance offset G_{D10} , peak heights δG_{D11} and δG_{D12} , peak locations ΔV_{G11} and ΔV_{G12} , and width scale factor a are adjusted in the fit. The fit to the conductance of Dot 2 in Fig. 4(b) (the ‘switching line shape’) was empirically made to two thermally smeared step functions:

$$G_{D2}(\Delta V_G) = G_{D20} + \frac{\delta G_{D20}}{2} \times ((1 + \tanh(b(\Delta V_G - \Delta V_{G21}))) - (1 + \tanh(b(\Delta V_G - \Delta V_{G22}))))),$$

where the conductance offset G_{D20} , step height δG_{D20} , switching locations ΔV_{G21} and ΔV_{G22} , and width scale factor b are adjusted in the fit. The $1 + \tanh()$ function may look unfamiliar, but it is simply the step function counterpart to the thermally smeared delta function $1/\cosh^2()$, and is obtained by integrating the delta function. The widths of the step functions used to fit

G_{D2} were constrained to be the same, as were their heights. As can be seen from Fig. 4, both functions fit the data well.

Figs. 5(a) and (b) show the conductances of Dots 1 and 2, respectively, as a function of side gate voltages ΔV_{G1} and ΔV_{G2} , zoomed in to the peak split region. For this measurement, Dot 1 was weakly tunnel coupled to its leads, resulting in narrow, thermally smeared Coulomb blockade peaks, while Dot 2 was strongly tunnel coupled to its leads, resulting in broad, lifetime-smeared peaks. Note, however, that the broad peaks of Dot 2 split abruptly (Fig. 5(b)) indicating that the switching line shape of Dot 2 is abrupt. On the other hand, the narrow peaks of Dot 1 ‘split’ smoothly (Fig. 5(a)) indicating that the switching line shape of Dot 2 is broad. This data emphasizes the fact that the abruptness of the switching line shape of the switched dot is controlled by how well quantized the charge on the trigger dot is.

Acknowledgements

This work was supported by DARPA grant DAAD19-01-1-0659, NSF grant DMR-98-0-2242 and NSF NSEC grant PHY-01-17795 at Harvard, and by the NSF QUEST Science and Technology Center at UCSB.

References

- [1] H. Grabert, M.H. Devoret (Eds.), Single Charge Tunneling, NATO ASI Series B: Physics, Vol. 294, Plenum Press, New York, 1992, and references therein.

- [2] L.L. Sohn, L.P. Kouwenhoven, G. Schön (Eds.), *Mesoscopic Electron Transport*, NATO ASI Series E: Applied Sciences, Vol. 345, Kluwer Academic Publishers, Boston, 1997, and references therein.
- [3] K.K. Likharev, *Single electron devices and their applications*, in: *Proceedings of IEEE (USA)*, Vol. 87, 1999, and references therein.
- [4] N.C. van der Vaart, S.F. Godijn, Y.V. Nazarov, C.J.P.M. Harmans, J.E. Mooij, L.W. Molenkamp, C.T. Foxon, *Phys. Rev. Lett.* 74 (1995) 4502.
- [5] F.R. Waugh, M.J. Berry, D.J. Mar, R.M. Westervelt, K.L. Campman, A.C. Gossard, *Phys. Rev. Lett.* 75 (1995) 705.
- [6] F. Hofmann, T. Heinzl, D.A. Wharam, J.P. Kotthaus, G. Böhm, W. Klein, G. Tränkle, G. Weimann, *Phys. Rev. B* 51 (1995) 13 872.
- [7] R.H. Blick, R.J. Haug, J. Weiss, D. Pfannkuche, K.v. Klitzing, K. Eberl, *Phys. Rev. B* 53 (1996) 7899.
- [8] C. Livermore, C.H. Crouch, R.M. Westervelt, K.L. Campman, A.C. Gossard, *Science* 274 (1996) 1332.
- [9] D. Dixon, L.P. Kouwenhoven, P.L. McEuen, Y. Nagamune, J. Motohisa, N. Sakaki, *Phys. Rev. B* 53 (1996) 12 625.
- [10] I.H. Chan, R.M. Westervelt, K.D. Maranowski, A.C. Gossard, *Appl. Phys. Lett.* 80 (2002) 1818.
- [11] D.S. Duncan, C. Livermore, R.M. Westervelt, K.D. Maranowski, A.C. Gossard, *Appl. Phys. Lett.* 74 (1999) 1045.
- [12] C. Livermore, D.S. Duncan, R.M. Westervelt, K.D. Maranowski, A.C. Gossard, *J. Appl. Phys.* 86 (1999) 4043.